Buckling Strength of Single-Angle Compression Members in K-Series Joists

JOSEPH ROBERT YOST, DAVID W. DINEHART, SHAWN P. GROSS, JOSEPH J. POTE, and JAMES DEENEY

Open web steel joists are prefabricated truss assemblies commonly used in roof and floor systems of lightly loaded structures. At the elemental level, joists are composed of a continuous top chord, continuous bottom chord, and diagonal web members. In many standard applications, the top and bottom chords are made of double angles and the web members are either circular bars, single crimped angles, or single uncrimped angles. Typical elevation and cross sections are shown in Figure 1, where it is noted that crimping the web angle eliminates the eccentricity between the web centroid and the centerline of the joist plane.

Definitions, design requirements, and associated standardized load tables are specified by the Steel Joist Institute (SJI) (SJI, 2002). Currently the SJI designates four joist series; (1) K-series; (2) longspan (LH); (3) deep longspan (DLH); and (4) joist girders. Joists are designated according to depth and span as follows: (1) K-series joists range in depth from 8 to 30 in. and spans to 60 ft; (2) LH-series joists range in depth from 18 to 48 in. and span up to 96 ft, and DLH-series joists range in depth from 52 to 72 in. and span up to 144 ft; and (3) joists girders range in depth from 20 to 72 in. and span up to 24 times the depth. This study explores the behavior of single-angle web members in K-series joists.

Capacity of the joist as a structural system is controlled by a limiting design strength in one of the three constituent members, or strength of the welds connecting the web and chord members. The top chord is typically in compression and continuously supported by a roof or floor slab so that flexural and flexural-torsional buckling is prevented. The bottom chord is typically in axial tension and supported at discrete intervals by transverse bridging. Design strength of the top chord is determined from interaction of axial compression and bending stresses. Top chord bending is due to transverse loading through the shear center and is about the member's weak axis. The bottom chord design strength is based on the member's yield capacity in axial tension.

Web design strength is dependent on bending effects that occur due to eccentricity of the axial force. When the angle is crimped and oriented as shown in Figure 1, the joist centerline and web centroid are coplanar. Accordingly, design strength of crimped compression web members is determined from concentrically loaded column analysis.

Joseph Robert Yost is associate professor, department of civil and environmental engineering, Villanova University, Villanova, PA.

David W. Dinehart is associate professor, department of civil and environmental engineering, Villanova University, Villanova, PA.

Shawn P. Gross is associate professor, department of civil and environmental engineering, Villanova University, Villanova, PA.

Joseph J. Pote is divisional director of engineering and head of research and development, SMI Joist, Inc., Hope, AR.

James Deeney is graduate assistant, department of civil and environmental engineering, Villanova University, Villanova, PA.

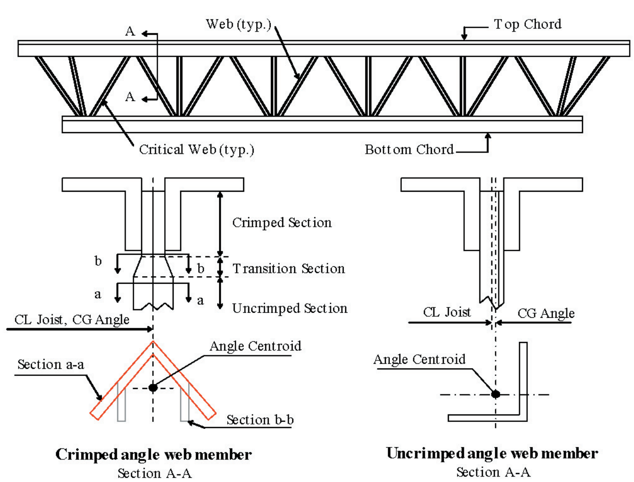

Fig. 1. Typical joist configurations.

However, for uncrimped web angles oriented as shown in Figure 1, bending effects must be considered due to the load eccentricity and design strength is derived from beam-column interaction. End conditions for both crimped and uncrimped web members are assumed to be pin connected at the chords. The connection welds are designed to resist at least two times the design load of the intersecting members (web and chord).

For eccentricities typical of uncrimped single-angle webs in open web steel joists, treatment of this member as a beam column results in a significant reduction in design strength relative to companion crimped members. However, based on research by Elgaaly, Dagher, and Davids (1991); Elgaaly, Davids, and Dagher (1992); Adluri and Madugula (1992); Gargan, Yost, Dinehart, and Gross (2002); and Deeney, Yost, Dinehart, and Gross (2003), the measured capacity of eccentrically loaded single-angle steel struts is significantly higher than that predicted by AISC load and resistance factor design (LRFD) interaction equations (AISC, 1999). These references note that simplifying assumptions related to end fixity and interaction strength and stability result in a significant underestimation of member capacity. Consequently, joist design strength limited by uncrimped web member capacity is overly conservative relative to measured behavior.

This paper outlines an experimental study conducted on K-series open web steel joists having crimped-end and uncrimped-end L1×1×7/64 in. structural angles for web members. The focus of the study is to compare measured strengths for crimped and uncrimped web members with design strengths calculated using existing analytical models. It is clear from the references cited that quantification of bending and end fixity must be more fully explored so that realistic analytical design models can be adopted. Measured strengths are compared with service and ultimate design strengths calculated using *SJI Standard Specifications, Load Tables, and Weight Tables for Steel Joists and Joists Girders* (SJI, 2002), which is in accordance with the AISC *Specification for Structural Steel Buildings, Allowable Stress Design and Plastic Design* (AISC, 1989), and *Load and Resistance Factor Design Specification for Single-Angle Members* (AISC, 2000), respectively. Also, bending in the critical web member is objectively quantified from measured strains through the cross section at mid-length.

SPECIMENS AND EXPERIMENTAL TEST SETUP

Experimental investigation included testing 18 simply supported, K-series joist samples, nine samples each with crimped and uncrimped single-angle web members. All samples spanned 15 ft 8 in. between support centerlines and the depth was either 18, 24, or 30 in. For each depth, three identical crimped and uncrimped samples were tested. Individual sample designation is of the form number followed by small cap followed by UCR or CR. The number is 18, 24, or 30 and represents the sample depth in inches, the small cap identifies an individual sample, and UCR and CR represent uncrimped and crimped web members, respectively. All joists have double angles 2L2×2×1/8 in. for the top and bottom chords, single angles L1×1×7/64 in. for the interior web members, and solid 7/8-in.-diameter round stock for the two exterior web members. Figures 2 and 3 depict sample and instrumentation details with all relevant sizes and dimensions. The single-angle web member slenderness (b/t) is 9.1. The local buckling limit on single-angle compression members is

$$0.446\sqrt{E/F_y}$$

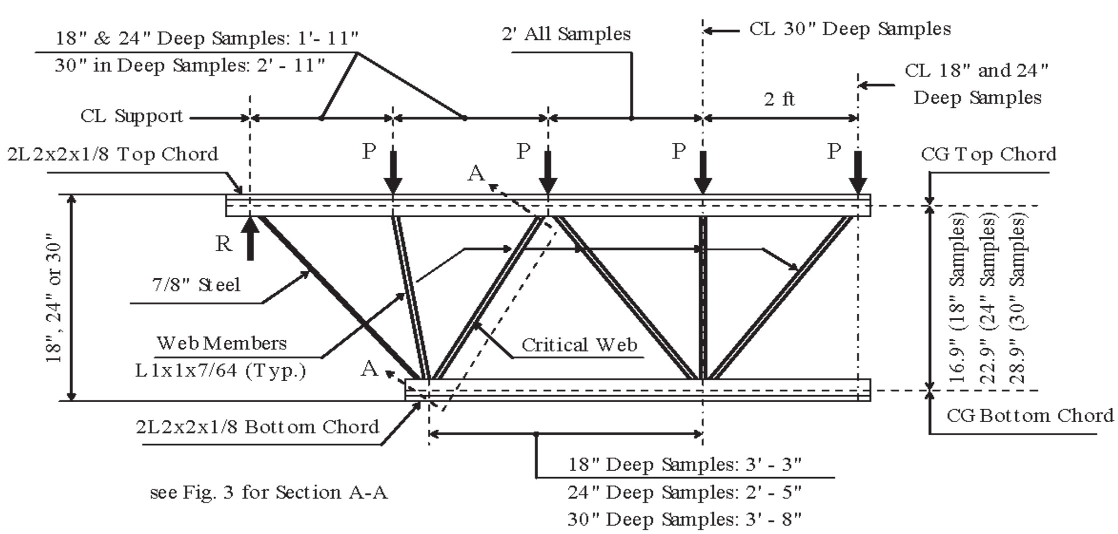

Fig. 2. Test sample details.

or

$$0.446\sqrt{29{,}000\,\text{ksi}/50\ \text{ksi}} = 10.74 \text{ (AISC, 2000)}$$

Thus, the interior web members are compact for local buckling, and the strength reduction factor, Q, may be taken as unity. The top chord was laterally braced at uniform intervals to prevent flexural and flexural-torsional buckling. Finally, all joists were configured so that buckling of the critical web would control strength.

To simulate a uniformly distributed force pattern, load was applied at each top chord panel point using hydraulic cylinders. Load was applied at an approximate rate of 1 kip/min and measured at the end panel points (left and right) using load cells. All hydraulic cylinders were connected to the same pump via distribution manifolds. Therefore, all cylinders had exactly the same hydraulic pressure and, hence, applied the same force to each loaded panel point. This was verified by having two load cells in the system and noting that each recorded identical loads for the duration of the test. Vertical displacement was measured at midspan on the bottom chord (Figure 2) using a linear variable differential transducer (LVDT). Axial strains in the critical webs (left and right) were measured with eight strain gages located at the web midspan as is shown in Figure 3. Strain data are used to evaluate axial force, internal bending, and end fixity. During testing, electronic signals from the two load cells, LVDT, and all strain gages were measured at a frequency of 1 Hz using a 16-bit data acquisition system.

All joist steel was designated ASTM A572 Grade 50, for which the elastic modulus (E) and minimum tensile yield stress (F_y) are specified as 29,000 and 50 ksi, respectively. The yield strength was experimentally investigated by uniaxial tension tests of coupon samples. Six tensile coupon samples were tested in accordance with ASTM E8-01 (ASTM, 2001) from which the as-tested average yield strength (F_y) was found to be 57 ksi.

DESIGN STRENGTH

Using a simplified truss analysis, the relationships between web axial force (P_{web}), number of loaded panel points (N), and the externally applied panel point load (P_{panel}) for the simply supported joist shown in Figure 4 is given as follows:

$$P_{web} = P_{panel}\,[(N/2) - 1]\,(L' / d_e) \tag{1}$$

Substituting N, L', and d_e from Figure 2 into Equation (1) yields P_{web}/P_{panel} for 18-, 24-, and 30-in.-deep joists of 3.34, 2.56, and 1.82, respectively. For design, the unknown in Equation 1 is P_{web}. The Steel Joist Institute (SJI) specifies P_{web} using allowable stress design (ASD) (SJI, 2002), where the SJI ASD design procedures are in accordance with the provisions specified in *Specification for Structural Steel Buildings, Allowable Stress Design and Plastic Design*, hereafter referred to as AISC-ASD (AISC, 1989). Again, column analysis and beam-column analysis are employed for crimped and uncrimped members, respectively. Cross-section geometry and assumed loading for uncrimped and crimped web members for the joists tested in this study are shown in Figure 5. For the uncrimped web members (Figure 5a), axial force (P_{web}) is assumed to be eccentric with respect to each of the principal centroidal axes and the member is analyzed as an eccentrically loaded pinned-end column. The

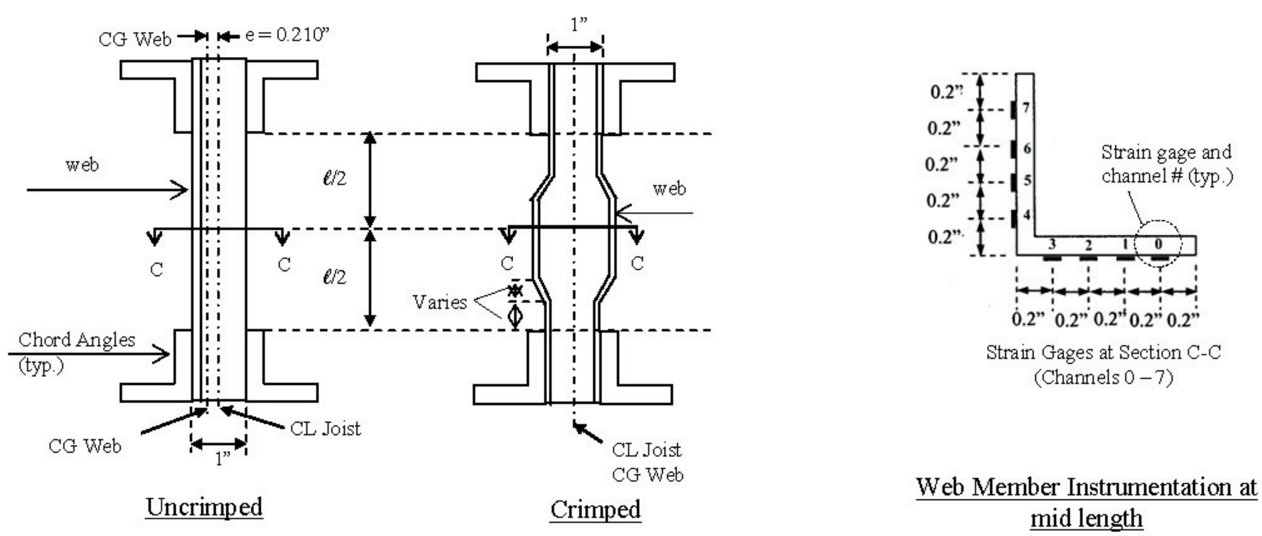

Fig. 3. Cross-section details.

ASD interaction design requirement applied to uncrimped web members is taken from SJI (2002), which is identical to AISC-ASD Chapter H, Section H1, Equation H1-1 (AISC, 1989) and given for biaxial bending as follows:

$$\frac{f_a}{F_a} + \frac{C_{mw}\, f_{bw}}{[1-(f_a/F'_{ew})]\,F_b} + \frac{C_{mz}\, f_{bz}}{[1-(f_a/F'_{ez})]\,F_b} < 1.0 \text{ Beam column ASD interaction} \tag{2}$$

where

f_a = axial compressive stress = P_{web}/A

f_{bw} = compressive stress at point a (Figure 5a) for moment about the w-axis
= $(P_{web}\, e_w\, c_{wa})/I_w$

f_{bz} = compressive stress at point a (Figure 5a) for moment about the z-axis
= $(P_{web}\, e_z\, c_{za})/I_z$

F'_{ew} = $(12\pi^2 E)/[23(kl/r_w)^2]$

F'_{ez} = $(12\pi^2 E)/[23(kl/r_z)^2]$

C_m = $1 - 0.40(f_a/F_e')$

F_b = allowable bending compressive stress
= 30 ksi (or $0.60F_y$)

F_a = allowable axial compressive stress found from SJI (2002) or AISC-ASD Chapter E, Equations E2-1 and E2-2 (AISC, 1989) and given for weak axis (z-axis) buckling as follows:

$$F_a = \frac{\left[1-[(kl/r_z)^2/(2C_c^2)]\right]QF_y}{5/3+(3/8)\left[(kl/r_z)/C_c\right]-(1/8)\left[(kl/r_z)/C_c\right]^3} \tag{3a}$$

for $kl/r_z \le C_c$

$$F_a = \frac{12\,\pi^2\,E}{23\,(kl/r_z)^2} \tag{3b}$$

for $kl/r_z > C_c$

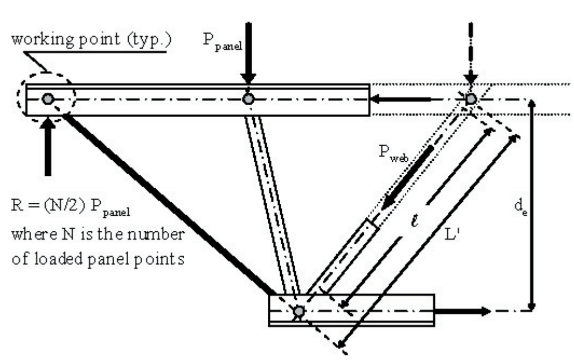

Fig. 4. Relationship between external load and web force.

where

l = clear member length measured between the chord angles (see Figure 4)

k = effective length factor = 1.0 (for assumed pinned end condition)

r_z = radius of gyration about the z-axis (weak axis)

A = member cross-sectional area

Q = reduction factor = 1.0

E = 29,000 ksi

F_y = 50 ksi (assumed for design)

C_c = $\sqrt{2\pi^2 E/QF_y}$

For the crimped-web member (Figure 5b), bending is assumed to be absent and the ASD interaction design requirement of Equation 2 reduces to the stress inequality $f_a < F_a$, where F_a is given in Equation 3. For joist chord and web members designed using the ASD method (Equations 2 and 3), SJI requires a minimum factor of safety (FOS) of 1.65 relative to experimentally measured member ultimate strength (SJI, 2002). This minimum FOS will be significant in later discussions.

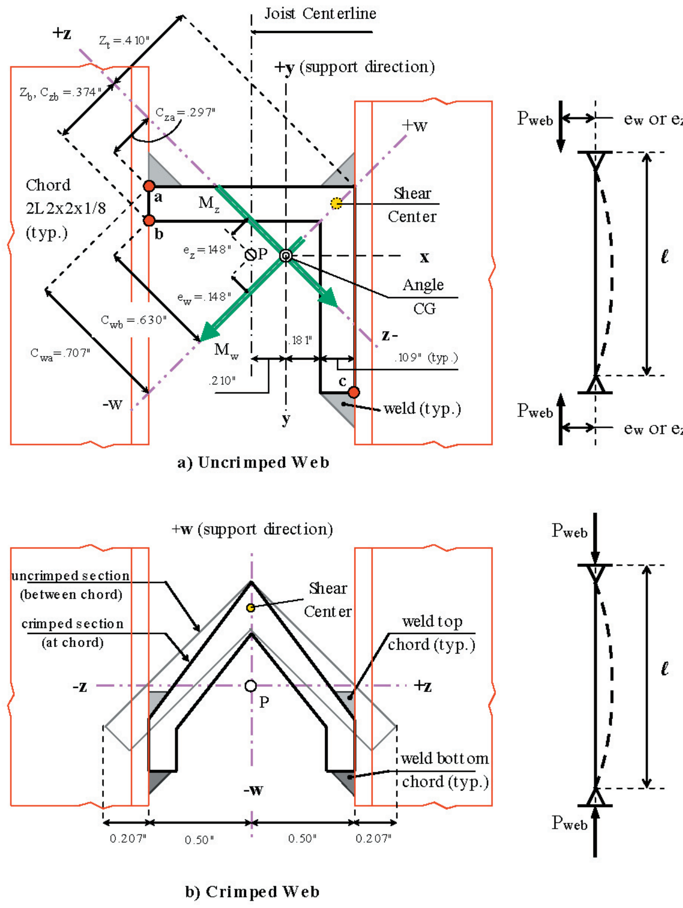

Fig. 5. Web member properties.

The theoretical interaction ultimate strength for uncrimped web members is calculated using the *Load and Resistance Factor Design Specification for Single-Angle Members* (AISC, 2000), Equations 6-1a and 6-1b, and expressed for biaxial bending as follows:

$$\frac{P_u}{\phi_c P_n} + \frac{8}{9}\left(\frac{M_{uw}}{\phi_b M_{nw}} + \frac{M_{uz}}{\phi_b M_{nz}}\right) \le 1.0$$
$$\text{for } \frac{P_u}{\phi_c P_n} \ge 0.2 \text{ Beam column LRFD interaction} \qquad (4a)$$

$$\frac{P_u}{2\phi_c P_n} + \left(\frac{M_{uw}}{\phi_b M_{nw}} + \frac{M_{uz}}{\phi_b M_{nz}}\right) \le 1.0$$
$$\text{for } \frac{P_u}{\phi_c P_n} < 0.2 \text{ Beam column LRFD interaction} \qquad (4b)$$

where

P_u = required axial strength = P_{web} at ultimate
P_n = nominal strength = $F_{cr}A$
M_u = required flexural strength = $B_1 P_{web} e$
B_1 = moment magnifier = $C_m / [1 - (P_u/P_{e1})] \ge 1$
P_{e1} = $\pi^2 EI/(kl)^2$
C_m = $0.60 - 0.40(M_1/M_2)$
M_1/M_2 = -1 for single curvature, equal end moments (Figure 5a)
M_n = nominal flexural strength for *point a*
= minimum of $M_{n\text{-}LB}$ (local buckling strength, M_w and M_z), $M_{n\text{-}yield}$ (yield strength when leg tips are in tension for M_z, therefore not applicable), and $M_{n\text{-}LTB}$ (lateral-torsional buckling strength, M_w only)
$M_{n\text{-}LB}$ = $1.5\ F_y\ S_{comp}$ [Reference: AISC (2000), Equation 5-2]
$M_{n\text{-}LTB}$ = $[0.92 - 0.17M_{ob}/M_y]M_{ob}$ for $M_{ob} \le M_y$ [Reference: AISC (2000), Equation 5-3a] or $[1.92 - 1.17\sqrt{M_y/M_{yob}}\,]M_y \le 1.5M_y$ for $M_{ob} > M_y$ [Reference: AISC (2000), Equation 5-3b]
M_{ob} = $C_b(0.46)Eb^2t^2/l$ (Reference: AISC (2000), Equation 5-5)
M_y = $F_y S_{ten}$
C_b = $12.5M_{max}/[2.5M_{max} + 3M_A + 4M_B + 3M_C]$
ϕ_c = ϕ_b = strength reduction factor for compression and bending, respectively
= 0.90

In P_n, F_{cr} is the critical flexural-buckling stress for axial loading given in AISC (2000), Equations 4-1 and 4-2 as follows:

$$F_{cr} = Q\left(0.658^{Q\lambda_c^2}\right) F_y \quad \text{for } \lambda_c\sqrt{Q} \le 1.5 \qquad (5a)$$

$$F_{cr} = \left[\frac{0.877}{\lambda_c^2}\right] F_y \qquad \text{for } \lambda_c\sqrt{Q} > 1.5 \qquad (5b)$$

where

Q = 1
λ_c = $(kl/\pi r_z)\sqrt{F_y/E}$ and ℓ, k, r_z, A, E and F_y are as in Equations 2 and 3.

For crimped members (Figure 5b), there is (theoretically) no bending and the LRFD interaction strength of Equation 5 reduces to axial force strength $P_u = \phi_c P_n$, where $P_n = F_{cr} A$ and F_{cr} is found from Equation 5.

ASD and LRFD design web strengths are summarized in Table 1. For the purpose of comparison with experimental strength, the LRFD strength reduction factors for bending (ϕ_b) and axial compression (ϕ_c) are taken as unity.

It is noted that the failure mechanism of flexural-torsional buckling (FTB) has been neglected as an ultimate limit state in the strength analysis presented above. Recognizing that the shear center does not coincide with the geometric centroid of the section, a torsional effect is possible for both crimped and uncrimped members. However, for web angles in this study, the FTB strength calculated according to LRFD Appendix E3, Equations A-E3-2, A-E3-3, and A-E3-6 (AISC, 1999) will not govern over the flexural-buckling strength of AISC (2000) given in Equation 5. Also, it has been suggested (Galambos, 1991) that, for design of angle columns, consideration of FTB as a limit state is more complicated than necessary. Galambos notes that based on experimental research from Kennedy and Murty (1972) and Kitipornchai and Lee (1986), AISC-LRFD minor axis buckling predicts shorter angle column strength conservatively.

TEST RESULTS

Load-deflection results are shown in Figure 6, where response is observed to be linear until failure. As expected, all samples failed due to buckling of one of the two (left or right) critical web members. Typical web buckling is shown in Figure 7. Buckling of the critical web member resulted in a sudden and significant drop in load-carrying capacity of the joist. For the joists tested, there was no appreciable post-failure load redistribution around the critical web, and all tests were terminated after web buckling. This behavior characterized all samples regardless of depth and web type as either crimped or uncrimped. It should be noted that in certain field situations where there is no limitation on vertical deformation, the bottom chord could bend at the next panel point and ultimately form a new longer stable panel mechanism. Thus, for this new panel mechanism, load can redistribute around the failed web member, but only after significant deformation. This behavior has been observed in failures of roof and floor joists where gravity loads deform the structure until this secondary mechanism forms. Test results are discussed in the following sections according to location of buckling, strength, and strain distributions.

Table 1. Summary of Design Loads and Test Results

			Analytical P_{web}		Measured At Failure				Factor of Safety			
Sample (-)	Web (type)	ℓ/r_z (-)	ASD [a] (k)	LRFD [b] (k)	P_{panel} (k)	P_{web} [c] (k)	avg. P_{web} (k)	CR/Ucr (-)	P_{web}/ASD (-)	P_{web}/LRFD (-)	P_{web} / CR ASD (-)	P_{web} / CR LRFD (-)
18l	Crimped (CR)	95.6	3.24	5.28	2.35	7.86	8.22	1.11	2.54	1.56		
18b					2.32	7.77						
18j					2.70	9.02						
18c	Uncrimp (UCR)		1.435	2.81	2.41	8.07	7.40		5.16	2.63	2.28	1.40
18d					2.14	7.16						
18k					2.09	6.98						
24e	Crimped (CR)	104.4	2.81	4.64	2.48	6.34	6.66	1.25	2.37	1.43		
24g					2.60	6.65						
24h					2.73	6.98						
24f	Uncrimp (UCR)		1.32	2.55	2.14	5.47	5.34		4.05	2.09	1.90	1.15
24j					1.93	4.94						
24k					2.19	5.60						
30a	Crimped (CR)	161.4	1.18	1.99	3.35	6.11	5.50	1.36	4.66	2.76		
30b					2.88	5.25						
30e					2.81	5.12						
30c	Uncrimp (UCR)		0.74	1.37	2.07	3.78	4.03		5.42	2.94	3.42	2.03
30d					2.34	4.27						
30f					2.22	4.05						

[a] Equations 2 and 3

[b] Equation 4 and 5 with $\phi_b = \phi_c = 1.0$.

[c] Equation 1

Buckled Locations

For all crimped 18-in.-deep samples, the critical web buckled near the crimp transition and the direction was primarily out of the plane of the joist (Figure 7a). Buckling occurred on the uncrimped side of the transition zone (Figure 7a) and was at the top crimp for samples 18b and 18l, and bottom crimp for sample 18j. Buckling at this location (near the crimp transition) is likely the result of a stiffness reduction and stress concentration that occurs as the angle transitions from the uncrimped to the crimped section. In all crimped 18-in.-deep samples, there was a clear bulging of the angle on the compression side at the buckled location (Figure 7a). This likely reflects local compression failure in the weak direction of the angle leg. Finally, the buckled shape for these members showed significant rotational restraint at the top and bottom joints.

For all uncrimped 18-in.-deep samples, critical web buckling occurred at or near midspan of the web member and was also directed primarily out of the plane of the joist (Figure 7b). The direction of lateral deformation clearly reflected weak axis buckling and, using the orientation shown in Figure 5a, occurred in the positive w-direction. This direction is to be expected and reflects that the minor-axis (z) load eccentricity is in the negative w-direction creating compression on the leg tips. As with the crimped 18-in.-deep samples, the buckled shape indicated significant rotational restraint at the intersections with the chords.

For all crimped and uncrimped 24- and 30-in.-deep samples, the critical web buckling occurred at or near midspan and was directed in the joist plane for crimped samples (Figure 7c) and out of the joist plane for uncrimped samples. No local failure at the crimp transition occurred. As with uncrimped 18-in.-deep samples, the buckled shape and direction of most 24- and 30-in.-deep samples suggests flexural buckling about the weak axis and considerable rotational restraint at the joints.

Strength and Factor of Safety

Measured failure loads are shown together with ASD and LRFD strengths in Table 1. Average measured strengths for crimped 18-, 24-, and 30-in.-deep web members are 11, 25, and 36%, respectively, greater than companion uncrimped web members. Results show that the increase in measured capacity associated with crimping is inversely proportional to slenderness. Thus, as expected, bending effects due to load eccentricity are more destabilizing in slender uncrimped members.

All measured failure loads exceed the required minimum SJI (SJI, 2002) strength of 1.65 times the allowable service load. Referring to Table 1, the factor of safety relative to the ASD design strength ranges for crimped members from 2.37 to 4.66, and for uncrimped members from 4.05 to 5.42. Regarding ultimate strength, the measured capacity at failure of all members is well in excess of their respective LRFD strength limits. Table 1 shows measured failure loads for crimped web members are between 1.43 and 2.76 times theoretical ultimate strengths. This ratio ranges from 2.09 to 2.94 for uncrimped web members.

In general, the factors of safety are greater for uncrimped members than for crimped members of like depth. Thus, the degree of conservatism in the beam-column model for uncrimped members is higher than in the column model for crimped members. In fact, the uncrimped member factor of safety based on ASD column analysis is between 1.90 and

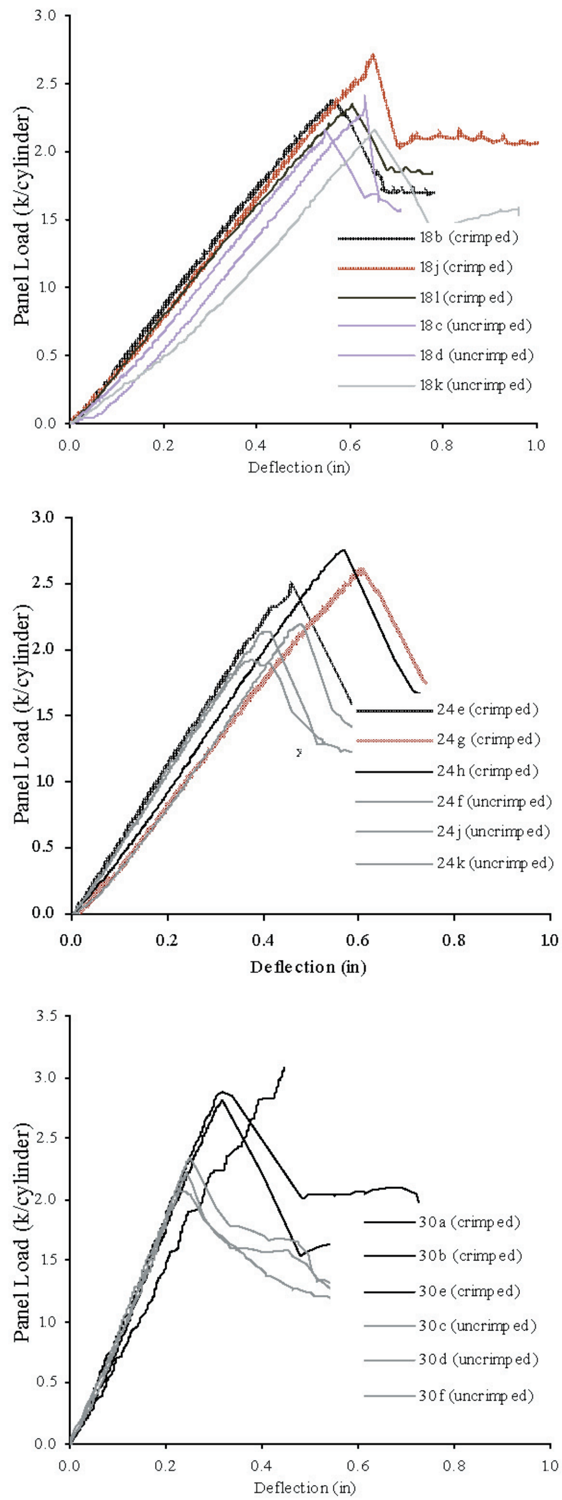

Fig. 6. Load deflection results.

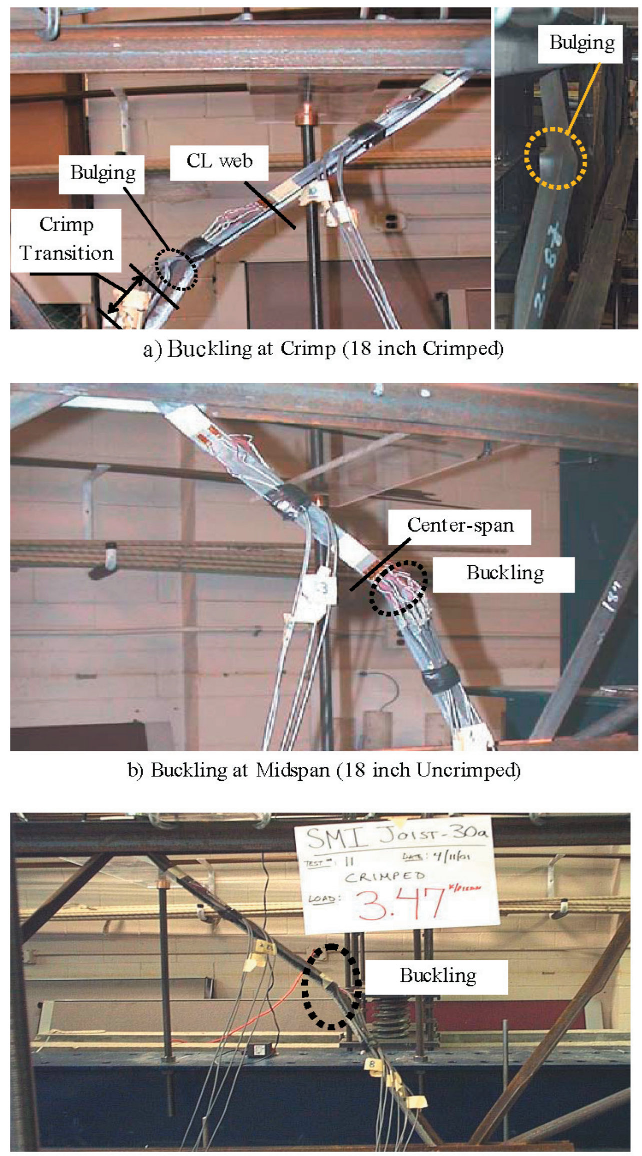

a) Buckling at Crimp (18 inch Crimped)

b) Buckling at Midspan (18 inch Uncrimped)

c) Buckling at Midspan (24 inch Crimped)

Fig. 7. Typical web buckling.

3.42. Also, the measured capacity of all uncrimped samples was greater than the LRFD analytical column design strength determined for crimped members (1.40, 1.15, and 2.03 in Table 1). The implication being that the existing analytical design strength for axial loading is overly conservative not only for the crimped members but also for the uncrimped members. This is in clear violation of the basic divergent treatment of column and beam column behavior for crimped and uncrimped sections, respectively.

Table 1 shows the measured factors of safety and ultimate strengths are significantly greater than minimum required ASD and LRFD limits, respectively, implying that current methods of analysis and associated boundary conditions do not reflect sufficiently well the actual behavior. The margins by which measured results exceed ASD and LRFD requirements is overly conservative and, consequently, review of bending and end fixity in Equations 2 through 4 is warranted. A detailed discussion of end fixity for the crimped members can be found in Yost, Dinehart, Gross, Pote, and Gargan (2004).

Strain Distribution

Typical strain distributions measured through the cross section at center span of crimped and uncrimped buckled (critical) web members for each joist depth are shown at approximately 0.50-kip intervals in Figure 8. At each load, the four strain readings on the left and right correspond to gages 0 through 3 and 4 through 7, respectively, as indicated in Figure 3. For reference, a pure axial condition in Figure 8 would be reflected by a horizontal line of constant strain. However, from Figure 8 the presence of bending is clearly evident and reflected in the strain gradient that occurs through the cross section. Bending is seen to occur in both the crimped and uncrimped webs, and the basic design assumption of axial loading for crimped web members is clearly not consistent with the strain distributions shown for crimped members in Figure 8. For the crimped web members strain magnitudes are higher at the leg tips and decreases with distance toward the angle heel. This shape suggests bending about the z-axis (Figure 5b). Also, the strain distributions in the uncrimped members are consistent with the assumed load location, P, shown in Figure 5a. That is, the net stress at point “a” in Figure 5a should be greater than the net stress at point “c” due to the additive effect of compression stresses from M_w and M_z. This expected result is substantiated in the uncrimped stress distributions of Figure 8.

Buckling near the crimp transition for the 18-in.-crimped samples is noted in Figure 8a for Sample 18b. As can be seen, for this sample the center-span strains do not become excessively large at failure, as is characteristic of all other samples. Referring to Figures 8b through 8f, when the member fails at center-span, the post-failure strains are all well in excess of $3{,}000 \times 10^{-6}$. This is a result of the severe distortion of the cross section at the location of buckling (midspan).

In summary, the results presented in Figure 8 show bending is present in the crimped web members and that crimped and uncrimped members are not that different relative to maximum measured strain magnitudes resulting from internal axial force and bending effects. Also, from Table 1, the LRFD limit state strengths for axial analysis (crimped members) and interaction analysis (uncrimped members) are overly conservative. In the following section, bending is quantified using measured strains and design assumptions are discussed.

INTERPRETATION OF STRAIN DATA

In the principal coordinate system, elastic stresses at any point in the cross section are calculated as the superposition of axial effects and bending effects about the major (w) and minor (z) axes. For three arbitrary points (i, j, k) within the member cross section, these stresses are calculated as follows:

$$\begin{bmatrix} \varepsilon_i E \\ \varepsilon_j E \\ \varepsilon_k E \end{bmatrix} = P_{web} \begin{bmatrix} \frac{1}{A} \\ \frac{1}{A} \\ \frac{1}{A} \end{bmatrix} + M_w \begin{bmatrix} \frac{z_i}{I_w} \\ \frac{z_j}{I_w} \\ \frac{z_k}{I_w} \end{bmatrix} + M_z \begin{bmatrix} \frac{w_i}{I_z} \\ \frac{w_j}{I_z} \\ \frac{w_k}{I_z} \end{bmatrix} \tag{6}$$

where

P_{web}, M_w, M_z = internal axial force, and bending moment about the strong and weak axes, respectively

A = member area (= 0.209 in.^{2})

I_w = moment of inertia about the weak (I_z = 0.0301 in.^{4}) axis

I_z = moment of inertia about the strong (I_w = 0.1904 in.^{4}) axis

z, w = coordinates in the principal coordinate system at a given location (i, j, k)

ε = strain at a given location (i, j, k)

E = modulus of elasticity = 29,000 ksi

From experimental data, ε at a given load level is known at eight different locations in the cross section at the critical web midlength (see Figure 3). As such, the unknowns in Equation 6 are the internal conditions P, M_w, and M_z. These unknowns are calculated in matrix form as follows:

$$\begin{bmatrix} P \\ M_w \\ M_z \end{bmatrix} = \begin{bmatrix} \frac{1}{A} & \frac{z_i}{I_w} & \frac{w_i}{I_z} \\ \frac{1}{A} & \frac{z_j}{I_w} & \frac{w_j}{I_z} \\ \frac{1}{A} & \frac{z_k}{I_w} & \frac{w_k}{I_z} \end{bmatrix}^{-1} \begin{bmatrix} \varepsilon_i E \\ \varepsilon_j E \\ \varepsilon_k E \end{bmatrix} \tag{7}$$

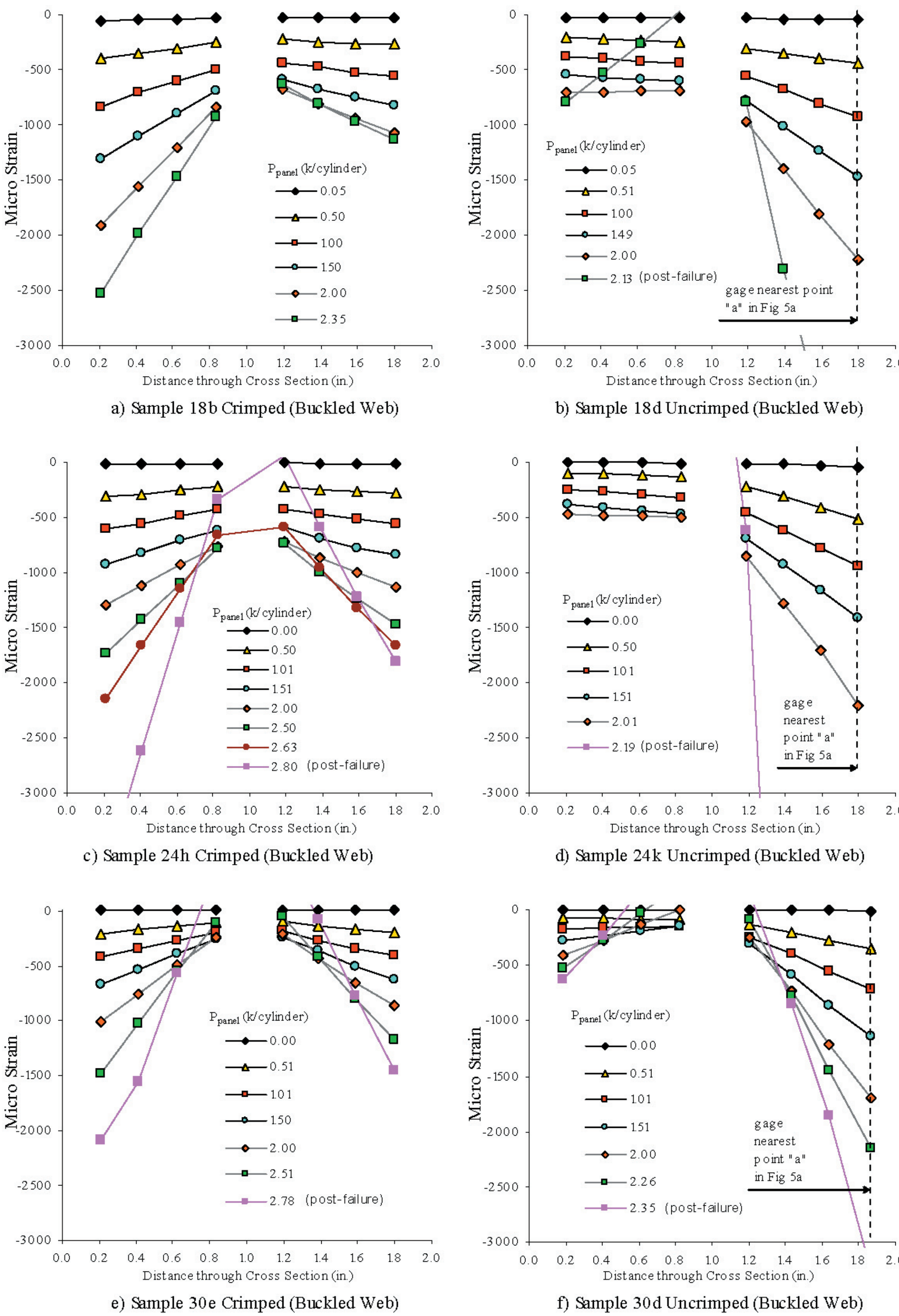

a) Sample 18b Crimped (Buckled Web)

b) Sample 18d Uncrimped (Buckled Web)

c) Sample 24h Crimped (Buckled Web)

d) Sample 24k Uncrimped (Buckled Web)

e) Sample 30e Crimped (Buckled Web)

f) Sample 30d Uncrimped (Buckled Web)

Fig. 8. Strain distribution at center span of critical web.

Recognizing that only three of eight strain magnitudes are required for a solution, multiple combinations exist to calculate P, M_w, and M_z. Of course, assuming a linear strain gradient on each leg, any combination of three should yield the same values for P, M_w, and M_z. Understandably, measured strain gradients on each leg of the web member are close but not exactly linear. For this reason, four different combinations of three points from the eight available were used to evaluate Equation 7 at a given cylinder load level. Then, the average of the four results for P_{web}, M_w, and M_z is used to represent the internal conditions of axial force and bending moment. Finally, knowing moments M_w and M_z, the resultant moment acting through the elastic centroid at a given load level is given as follows:

$$M_r = \sqrt{M_w^{\ 2} + M_z^{\ 2}} \tag{8}$$

Because the analysis is only valid for elastic behavior, results are limited to cylinder loads of 2 kips, at which all measured strains are within the elastic range. The resultant moment in the web was computed at 0.50 kip intervals up to 2 kips per cylinder and is shown in Figure 9.

Referring to Figure 9, measured results show there is bending in both crimped and uncrimped web members. In general, bending in crimped web members is less than that in uncrimped web members of equal length. As such, crimping does reduce the effects of bending due to load eccentricity but does not eliminate it. The increase in bending moment for uncrimped web members is more pronounced in the 24- and 30-in.-deep joist samples than for the 18-in.-deep joist samples. This behavior, in part, reflects the increased transverse deflection and associated increased P-Δ bending that occurs in longer, uncrimped compression webs.

In conclusion, the basic assumption of column action and beam-column action governing the design of crimped and uncrimped web members, respectively, is not justified from the results presented. Rather, for K-series joists it appears more logical to treat all members (crimped and uncrimped) as axially loaded columns and account for bending moments that occur from the inevitable load eccentricity by a simpler empirical mechanism.

DISCUSSION

In routine structural design, compression strength is mathematically modeled using simplified empirical procedures. The empirical form reflects difficulties in modeling the true conditions related to load, support, and member characterization. Specifically, the exact conditions related to load eccentricity, residual stress, initial imperfection, end restraint, and deflected shape under load are never known. This is especially true for single-angle web members in K-series joists where fabrication tolerances related to web orienta-

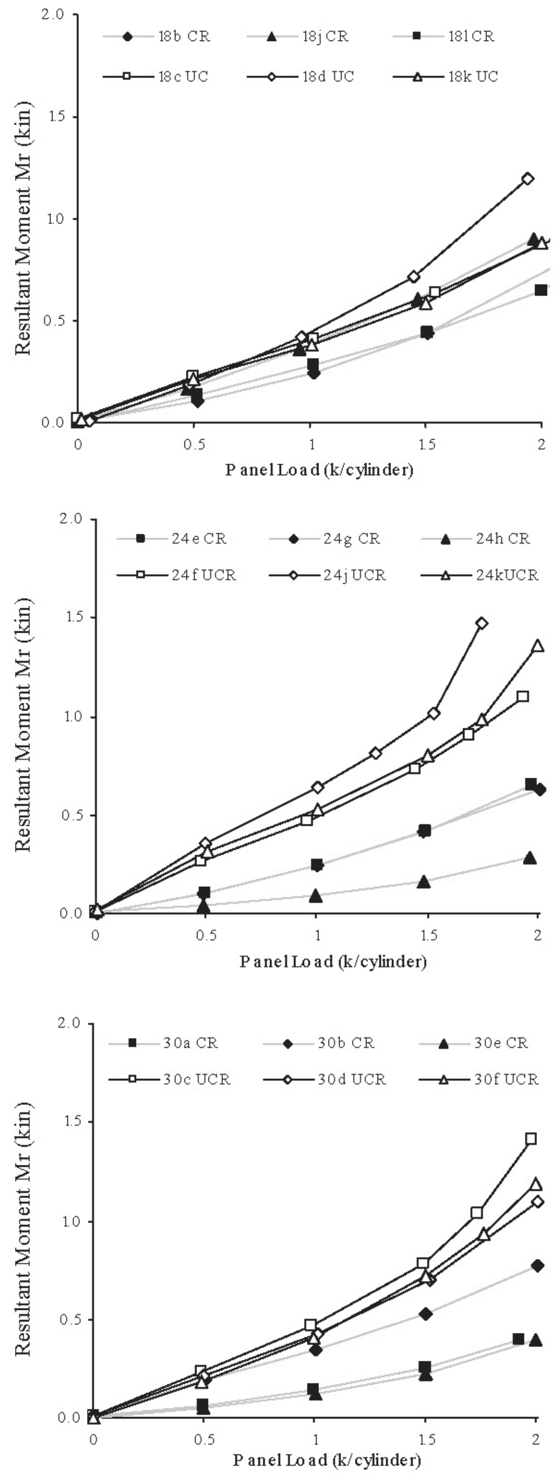

Fig. 9. Internal bending results.

tion, weld size and location, and crimping geometry are always different from the idealized conditions of Figures 3, 4, and 5. More realistically, for web members in steel joists conditions related to load location, member orientation, and end fixity will vary from sample-to-sample.

The simplified empirical analysis is recognized in Equations 2 through 5, where design web forces and stresses are determined for a given set of assumed boundary conditions. It has been shown that AISC LRFD interaction analysis produces reasonable and conservative agreement between measured and predicted limit state strengths of doubly symmetric framed compression members (Cai, Liu, and Chen, 1991). However, when these methods and boundary conditions are applied to crimped and uncrimped web members in K-series open web steel joists, this research, and that of others, has shown that member capacity is unacceptably conservative.

It is noted that in this study test samples were loaded at the panel points only. As a result there was no top chord moment induced by transverse loading. This load case is different from the continuous uniform loading of the top chord as is typically assumed in the SJI strength tables. However, for standard joists with equal span top chord lengths, the net web moment should be approximately the same for both the point load and continuous uniform load cases. This is due to a canceling effect of transverse load induced top chord moments on either side the panel point. For unbalanced loading of the top chord, however, moment would be expected in the web and this could potentially affect end fixity and strength.

Ultimately, the results of Table 1 justify modifications to current design assumptions related to end fixity and beam column interaction. However, such changes should consider more complete experimental data covering a wider range of loading conditions, in particular that of uniform loading of the top chord.

CONCLUSION

The following conclusions are made from the research reported in this study. It is understood that these conclusions are restricted to K-series steel joists subjected to panel point loads and having single angle L1×1×7/64 in. crimped and uncrimped web members and double angle 2L2×2×1/8 in. chord members.

1. Crimping the web angles increases the member's compression strength between 11 and 36% relative to companion uncrimped strength.

2. The current SJI-mandated column analysis (SJI, 2002) with an effective length factor of 1.0 for crimped angle web members is overly conservative. Measured failure loads are between 1.43 and 2.76 times theoretical LRFD ultimate strengths, and the factor of safety relative to ASD methodology ranges from 2.37 to 4.66.

3. The current SJI mandated beam column analysis (SJI, 2002) with an effective length factor of 1.0 for uncrimped angle web members is overly conservative. Measured failure loads are between 2.09 and 2.94 times theoretical LRFD ultimate strengths, and the factor of safety relative to ASD methodology ranges from 4.05 to 5.42.

4. Using column analysis, the ASD factor of safety for uncrimped web members ranges from 1.90 to 3.42, and measured failure loads are between 1.15 and 2.03 times analytical column LRFD ultimate strength.

5. Based on measured strains at midspan, internal bending is present in crimped web members. However, as expected, measured internal bending for uncrimped web members is greater than that for companion crimped web members.

Collectively, these conclusions suggest that current treatment of end fixity and beam column interaction is overly conservative, and modification to existing design methodology is warranted. However, the behavior reported in this research needs to be investigated for a wider range of joint stiffnesses and loading conditions. Specifically, additional testing on a wider range of web and chord sizes is recommended, and the effects of continuous uniform loading and unbalanced uniform loading of the top chord also needs to be investigated in future research studies.

NOTATION

A = angle cross-sectional area

c_w, c_z = perpendicular distance from the w and z axes, respectively, to any point in the cross section

C_c = AISC allowable stress design (ASD) axial compressive stress term

C_{mw}, C_{mz} = AISC ASD interaction terms for bending about the w and z axes, respectively

d_e = joist depth measured between chord centroids

e_w, e_z = load eccentricity with respect to the w and z axes, respectively

E = elastic modulus = 29,000 ksi

f_a = axial compressive stress = P_{web}/A

F_a, F_b = allowable axial compressive stress and allowable bending stress, respectively

f_{bw}, f_{bz} = bending stress for moment about the w and z axes, respectively

F_{cr}, F_y = critical buckling stress and yield stress, respectively

F'_{ew}, F'_{ez} = AISC ASD interaction terms for bending about the w and z axes, respectively

I_w, I_z = moment of inertia with respect to the w and z axes, respectively

k = effective length factor

l = clear web member length measured between the chord angles

L' = member length measured between working points

M_{nw}, M_{nz} = nominal flexural strength for bending about the w and z axes, respectively

M_{uw}, M_{uz} = required flexural strength for bending about the w and z axes, respectively

M_r = resultant moment from bending moments about the w and z axes

N = number of load points

P_{web}, P_{panel} = axial force in web and applied panel point load, respectively

P_u, P_n = required axial strength and nominal axial strength, respectively

Q, r = reduction factor for local buckling and radius of gyration, respectively

w, z = subscripts relating to strong and weak axes, respectively

ϕ_b, ϕ_c = strength reduction factors for flexure and axial compression, respectively

λ_c = AISC LRFD critical buckling stress term

ACKNOWLEDGMENTS

The authors wish to thank SMI Joist for supplying test specimens and financial support for conducting this research. Also the efforts of undergraduate research assistants and laboratory technician George Pappas are recognized and greatly appreciated.

REFERENCES

Adluri, M.R. and Madugula, M.K. (1992), "Eccentrically Loaded Steel Single Angle Struts," *Engineering Journal*, AISC, Vol. 21, No. 2, 2nd Quarter, pp. 59–66.

AISC (1999), *Load and Resistance Factor Design Specification for Structural Steel Buildings*, 3rd Edition, American Institute of Steel Construction, Inc., Chicago, IL.

AISC (1989), *Manual of Steel Construction, Allowable Stress Design,* 9th Edition, American Institute of Steel Construction, Inc., Chicago, IL.

AISC (2000), *Load and Resistance Factor Design Specification for Single-Angle Members*, American Institute of Steel Construction, Inc., Chicago, IL, November 10.

ASTM (2001), "Standard Test Methods of Tension Testing of Metallic Materials," ASTM E8-01, West Conshohocken, PA.

Cai, C.S., Liu, X.L., and Chen, W.F. (1991), "Further Verification of Beam-Column Strength Equations," *Journal of Structural Engineering*, ASCE, Vol. 117, No. 2, pp. 501–513.

Deeney, J., Yost, J.R., Dinehart, D., and Gross, S.P. (2003), "Strength and Deflection of Steel Joists with Un-Crimped, Crimped, and Full-Crimped Web Members," *Research Report #005 submitted to SMI Steel Products, Inc.*, Hope, AR.

Elgaaly, M., Dagher, H., and Davids, W. (1991), "Behavior of Single-Angle-Compression Members," *Journal of Structural Engineering*, ASCE, Vol. 117, No. 12, pp. 3720–3741.

Elgaaly, M., Davids, W., and Dagher, H. (1992), "Non-Slender Single Angle Struts," *Engineering Journal*, AISC, Vol. 21, No. 2, 2nd Quarter, pp. 49–58.

Galambos, T.V. (1991), "Design of Loaded Compression Angles," *Proceedings of the Structural Stability Research Council Technical Session*, April 15–17, Chicago, IL, pp. 353–367.

Gargan, B., Yost, J.R., Dinehart, D., and Gross, S.P. (2002), "Performance of Open Webbed Steel Joists With Crimped and Uncrimped Web Members," *Research Report #003 submitted to SMI Steel Products, Inc.*, Hope, AR.

Kennedy, J.B. and Murty, M.K. (1972), "Buckling of Steel Angle and Tee Struts," *Journal of the Structural Division*, ASCE, Vol. 98, No. ST11, pp. 2507–2522.

Kitipornchai, S. and Lee, H.W. (1986), "Inelastic Experiments on Angle and Tee Struts," *Journal of Construction Steel Research*, Elsevier, Vol. 6, pp. 219–236.

SJI (2002), *Standard Specifications, Load Tables, and Weight Tables for Steel Joists and Joist Girders*, Steel Joist Institute, Myrtle Beach, SC.

Yost, J.R., Dinehart, D.W., Gross, S.P., Pote, J., and Gargan, B. (2004), "Strength and Design of Open Web Steel Joists with Crimped-End Web Members," *Journal of Structural Engineering*, ASCE, Vol. 130, No. 5, May, pp. 715–724.